

1 **Combining serological assays and official statistics to describe the trajectory of the COVID-19**
2 **pandemic: results from the EPICOVID19-RS study in Rio Grande do Sul (Southern Brazil)**

3

4 Fernando P. Hartwig^{1*}, Luís Paulo Vidaletti², Aluísio J. D. Barros^{1,2}, Gabriel D. Victora³, Ana M.
5 B. Menezes¹, Marília A. Mesenburg^{1,4}, Bernardo L. Horta¹, Mariângela F. Silveira¹, Cesar G.
6 Victora^{1,2}, Pedro C. Hallal¹, Claudio J. Struchiner⁵

7

8 ¹Postgraduate Program in Epidemiology, Federal University of Pelotas, Pelotas, Brazil.

9 ²International Center for Equity in Health, Federal University of Pelotas, Pelotas, Brazil.

10 ³Laboratory of Lymphocyte Dynamics, Rockefeller University, New York, NY, United States.

11 ⁴Federal University of Health Sciences of Porto Alegre, Porto Alegre, RS, Brazil.

12 ⁵Getúlio Vargas Foundation, Rio de Janeiro, Brazil.

13

14 *Corresponding author. Postgraduate Program in Epidemiology, Federal University of Pelotas,
15 Pelotas (Brazil) 96020-220. Phone: +55 (53) 3284-1300. E-mail: fernandophartwig@gmail.com.

16

17 **ABSTRACT**

18 **Background:** The EPICOV19-RS study conducted 10 population-based surveys in Rio Grande
19 do Sul (Southern Brazil), starting early in the epidemic. The sensitivity of the rapid point-of-
20 care test used in the first eight surveys has been shown to decrease over time after some
21 phases of the study were concluded. The 9th survey used both the rapid test and an enzyme-
22 linked immunosorbent assay (ELISA) test, which has a higher and stable sensitivity.

23 **Methods:** We provide a theoretical justification for a correction procedure of the rapid test
24 estimates, assess its performance in a simulated dataset and apply it to empirical data from
25 the EPICOV19-RS study. COVID-19 deaths from official statistics were used as an indicator of
26 the temporal distribution of the epidemic, under the assumption that fatality is constant over
27 time. Both the indicator and results from the 9th survey were used to calibrate the temporal
28 decay function of the rapid test's sensitivity from a previous validation study, which was used
29 to estimate the true sensitivity in each survey and adjust the rapid test estimates accordingly.

30 **Results:** Simulations corroborated the procedure is valid. Corrected seroprevalence estimates
31 were substantially larger than uncorrected estimates, which were substantially smaller than
32 respective estimates from confirmed cases and therefore clearly underestimate the true
33 infection prevalence.

34 **Conclusion:** Correcting biased estimates requires a combination of data and modelling
35 assumptions. This work illustrates the practical utility of analytical procedures, but also the
36 critical need for good quality, populationally-representative data for tracking the progress of
37 the epidemic and substantiate both projection models and policy making.

38

39 **KEYWORDS:** COVID-19; SARS-CoV-2; seroprevalence; bias correction.

40 **1. INTRODUCTION**

41 Brazil concentrates 10% of all COVID-19 deaths in the world while having only 2.7% of the
42 world's population. As of February 28, 2021, Brazil is the country ranking second and third in
43 terms of deaths and confirmed cases, respectively. The situation was worsened the rapid
44 spread of a new variant of the SARS-CoV-2 virus in the Amazon region in the North(1), which is
45 already circulating in other regions of the country, including the South region(2). Rio Grande
46 do Sul (the Southernmost state in Brazil) is facing the worst situation since the start of the
47 pandemic, with infections increasing at unprecedented rates. In February 27 2021, all
48 subregions of the state were, for the first time, classified as being in a critical situation based
49 on a controlled social distancing model that uses several indicators and was launched by the
50 State's Government in May 2020(3).

51 Rio Grande do Sul was one of the first regions in the world to have a large population-based
52 assessment of the COVID-19 epidemic. According to official statistics, the first case and the
53 first death in the State occurred in February 29 and March 24, 2020, and the first of a series of
54 10 serological surveys (collectively referred to as the EPICOVID19-RS study(4)) in the State was
55 caried out in April 11-13, 2020(5). Although a series of surveys starting so early on is useful for
56 accurately tracking the progression of the epidemic, tests then available that were suitable for
57 population-based studies had only been tested in recently infected individuals. In the
58 EPICOVID19-RS study, a rapid point-of-care test was used. Prior to the 1st survey, available
59 validation studies indicated the test's performance was sufficiently high for population-based
60 studies(6). However, future validation studies detected that the sensitivity of this test
61 decreases over time(7), an assessment that was only possible after some time since the
62 beginning of the pandemic. In the 9th survey, we used an enzyme-linked immunosorbent assay
63 (ELISA), which has higher sensitivity than the rapid test that does not decrease over time⁷⁻⁸.
64 Changing tests between surveys hampers comparing different surveys, thus requiring
65 analytical procedures to properly utilize previous estimates based on the rapid test in
66 combination with the ELISA test to obtain a coherent picture of the pandemic in the state.

67 External data are extremely useful to furnish procedures to correct biased estimates. The more
68 data the lower the need for modelling assumptions. Typically, such data stems from official
69 statistics, such as registered cases, deaths, hospitalizations and other indicators. However,
70 such data have their own limitations, including dependence of testing policies and protocols,
71 fatality rate, change in treatment protocols, incompleteness and other factors that may
72 change both over time and among different locations.

73 Obtaining a coherent and likely more accurate temporal trend of how the epidemic in a given
74 location using real data is therefore a challenging task, requiring simultaneously and
75 coherently using different and imperfect sources of data, including official statistics, different
76 diagnostic tests and information from validation studies. This paper aims at obtaining the
77 cumulative prevalence of infection in Rio Grande do Sul from a series of nine population-based
78 serological surveys using a test with temporal variation in sensitivity.

79 **2. METHODS**

80 **2.1. Theoretical justification for the correction procedure**

81 Let $F(t) = \int_0^t f(x) dx$ denote the cumulative number of infections at time t , where $f(x)$ is a
82 non-zero function for the infection incidence (in number of new cases) and $t = 1$ is the day of
83 the first infection, so that $F(1) \geq 1$ and $F(t) = 1$ for some $t \in (0,1]$. Let $g(t^*) \in [0,1]$ denote

84 a function for the proportion of infections detectable t^* days after occurring. Therefore,
 85 $W(t) = \int_0^t f(x)g(t-x) dx$ represents the cumulative number of infections detectable at
 86 time t . We assume the population size N is constant throughout the pandemic. In this case,
 87 $\frac{F(t)}{N}$ and $\frac{W(t)}{N}$ respectively denote the true and apparent (detectable) cumulative prevalence of
 88 infections at time t .

89 From the notation above, the proportion of infections that are still detectable (i.e., the
 90 sensitivity) in day t is:

$$91 \quad D(t) = \frac{W(t)}{F(t)} = \frac{\int_0^t f(x)g(t-x) dx}{\int_0^t f(x) dx} \quad (1).$$

92 Equation 1 can be interpreted as a weighted average of the proportion of detectable
 93 infections, where the weights correspond to the number of infections that occurred in each
 94 short interval $[t, t + dt]$, where dt is a very small positive number.

95 Let $h(t) = cf(t) \Rightarrow H(t) = cF(t)$, where c is an unknown positive constant. $h(t)$ can
 96 denote, for example, the number of deaths, assuming that fatality is constant over time. In this
 97 case, t represents the time when the infection happened, so that $h(t)$ denote the number of
 98 new cases which ended up dying. If $h(t)$ denotes the number of deaths in time t , then the
 99 appropriate representation would be $h(t-k) = cf(t)$, where k denotes the number of days
 100 between infection and death.

101 Substituting $h(t)$ for $f(t)$ in equation 1 yields:

$$102 \quad \frac{\int_0^t h(x)g(t-x) dx}{\int_0^t h(x) dx} = \frac{\int_0^t cf(x)g(t-x) dx}{\int_0^t cf(x) dx} = \frac{\int_0^t f(x)g(t-x) dx}{\int_0^t f(x) dx} = D(t).$$

103 That is, the proportion of infections that are still detectable t^* days after occurring can also be
 104 obtained using any indicator of the temporal distribution of infections, assuming that such
 105 indicator is a scaled version of $F(t)$.

106 If both that $g(t^*)$ and some function $H(t)$ are known, $g(t^*)$ can used to account for the decay
 107 in sensitivity over time, and $H(t)$ can used to account for the temporal distribution of the
 108 pandemic. However, in practice, typically only $H^\#(t) = \sum_{x=1}^t h^\#(x)$, where $h^\#(x)$ is the
 109 number of deaths that occurred in a given day, is known. From this definition, $h^\#(t) =$
 110 $H(t-1) - H(t) = \int_{t-1}^t h(x) dx$ and $H^\#(t) = H(t)$ for $t \in \mathbb{N}^*$. Since the exact time of the
 111 events within a day are unknown, an approximation can be made by assigning $t^* = t^s - t$ to
 112 all events that happened in day t , where t^s denotes the date when individuals were tested.
 113 This is a good approximation because the $g(t^*)$ is unlikely to substantially change within a day
 114 – that is, $g(t^*) \approx g(t^* + 1)$.

115

116 From the above, $D(t)$ and $F(t)$ can be approximated as follows:

$$D(t) \approx \bar{D}(t) = \frac{\sum_{x=1}^t h^\#(x) \hat{g}(t-x)}{\sum_{x=1}^t h^\#(x)} \quad (2)$$

$$F(t) \approx \bar{F}(t) = \frac{\hat{W}(t)}{\bar{D}(t)} \quad (3)$$

117 Similar to $D(t)$ in equation 1, $\bar{D}(t)$ in equation 2 can be interpreted as a weighted average of
118 the proportion of detectable infections, where the weights correspond to the number of
119 infections that occurred in each day.

120 In practice, $h^\#(x)$ can be obtained from official statistics. However, the assumption that c is
121 constant over time is required for equation 2 to yield a good approximation of $F(t)$. If this is
122 not the case, then c should be replaced with $c(t)$. Moreover, it is unlikely that $g(t^*)$ is known
123 in practice. However, it can be estimated, for example, in validation studies. Therefore, $\hat{g}(t^*)$
124 is included in equation 2 instead of $g(t^*)$. Finally, equation 3 includes $\hat{W}(t)$, which is the
125 estimated apparent cumulative number of infections estimated using a test with sensitivity
126 that decreases over time, according to $g(t^*)$.

127 2.2. Simulation study

128 For the simulations, $f(t) = e^{-0.0002t^2 + 0.0848t}$, thus yielding ~1 million individuals who got
129 infected at some point during a one-year period. The population size was 11 million
130 individuals. Fatality rate was 1% and constant over time. These numbers are roughly of
131 comparable magnitude to the first year of the epidemic in Rio Grande do Sul.

132 Individual i (where i denotes a generic individual who was infected at some point) was
133 detectable by the Wondfo test at time t if $T_{1i} + T_{2i} + T_{3i} \leq t < T_{1i} + T_{2i} + T_{3i} + T_{4i}$, where:

- 134 • T_1 is the infection date (defined as described above).
- 135 • $T_2 \sim \text{Weibull}(\frac{1}{0.11}, 1.97)$ is the incubation time⁹⁻¹⁰.
- 136 • $T_3 \sim N(13.3, 32.49)$ is the time from symptom onset to seroconversion(11).
- 137 • $T_4 \sim \text{Weibull}(68.383320, 1.183745)$ is the time from seroconversion to seroreversion(12).
- 138 • T_5 is the time from symptom onset to diagnosis. This was estimated using official statistics
139 (see below for a description of these data) as the time difference between the dates of
140 diagnosis and of symptom onset. For the present analyses, values greater than 21 days
141 were discarded.

142 Regarding fatality, 1% of the infected individuals were randomly selected as those who died.
143 To define when individuals died, we defined the following transition times:

- 144 • T_6 is the time from diagnosis to death. This was estimated using official statistics (see below
145 for a description of these data) as the time difference between the dates of death and of
146 diagnosis.

147 Among individuals who died in the simulation study, values for $T_5 - T_6$ were generated by
148 sampling from their empirical joint distribution obtained from official statistics, restricting to
149 those diagnosed with RT-PCR and died. For individuals who did not die in the simulation study
150 T_5 values were generated by sampling from official statistics, restricting to those diagnosed
151 with RT-PCR and did not die. Therefore, this sampling scheme allows for violations of the
152 assumption that such times are similar between these subgroups. This may introduce some
153 bias in the corrected estimates, and the simulation study will help to quantify how much this
154 bias is likely to affect empirical analysis.

155 If individual i is one of those who died, if $t \geq T_{1i} + T_{2i} + T_{5i} + T_{6i}$, then the i th individual was
156 deceased at time t . Of note, all times were rounded to the nearest integer, and negative
157 values in T_3 were replaced with zero.

158 In the simulations, the population size decreases over time as infected individuals die. Deaths
159 due to other causes were not considered because we assumed that, aside from the epidemic,
160 the population size is constant over time. The parameter of interest is $\frac{F(t)}{N}$, where N is assumed
161 to be constant over time. Therefore, this is another source of (likely slight bias) in the
162 estimates, and such bias will be quantified in the simulations.

163 To generate $g(t^*)$, a hypothetical validation study involving 20 million individuals, all enrolled
164 in the day they were infected and each followed up for 400 days, was simulated by
165 independently sampling 20 million values for T_2 - T_4 from their respective distributions.
166 Therefore, if $T_{2i} + T_{3i} - T_{5i} \leq t^* < T_{2i} + T_{3i} + T_{4i}$, then individual i is detectable t^* days
167 after diagnosis. $g(t^*)$ was then defined as the proportion of individuals detectable t^* after
168 diagnosis. Such large validation study essentially implies that there is negligible error due to
169 sampling variability in $\hat{g}(t^*)$, such that $\hat{g}(t^*) \approx g(t^*)$.

170 We simulated a scenario of 4 population based serological surveys conducted at days $t = 60$,
171 $t = 120$ and $t = 180$ and $t = 240$. For each survey, 5000 individuals were randomly sampled
172 from the population. A total of 1000 datasets were simulated by sampling T_2 - T_6 from their
173 respective distributions and randomly allocating these values to the dataset of infected
174 individuals.

175 The correction procedure was implemented as an iterated procedure. In each dataset, 2000
176 iterations of the correction procedure for each survey were applied. In each iteration, $H^\#(t)$
177 values for T_2 were sampled from its distribution. These were subtracted from the date of
178 symptom onset, which is assumed to be known for each death (as in our empirical application).
179 This yields a distribution of when individuals who died were infected, which is a valid indicator
180 of the relative temporal distribution of all infections under the assumption that fatality rate is
181 constant over time. This relative temporal distribution, in combination with the sensitivity
182 function $g(t^*)$, was then used to calculate $\bar{D}(t)$ and $\bar{F}(t)$.

183 **2.3. Data sources**

184 **2.3.1. EPCOVID19-RS study**

185 The EPICOVID19-RS study is a series of 10 large, population-based surveys aiming at tracking
186 the COVID-19 pandemic in Rio Grande do Sul. For this paper, only surveys 1 to 9 will be used.
187 Data collection for the 1st and 9th surveys occurred in April 11-13 2020 and February 5-7 2021,
188 respectively. The study involves nine sentinel cities – that is, the largest city from each one of
189 the eight intermediate regions of the state as defined by the Brazilian Institute of Geography
190 and Statistics (IBGE). The exception was the metropolitan region, for which two cities (the
191 state capital and an additional city) were selected. In each city, 50 census tracts (delimited
192 areas with approximately 300 households each in urban area, also defined by the IBGE) were
193 selected with probability proportional to size and ensuring geographical representativity. In
194 each tract, 10 households were systematically selected. Between surveys, different households
195 were selected within the same tracts. One individual per households was randomly selected
196 for interview and testing using the rapid point-of-care lateral-flow WONDFO SARS-CoV-2
197 Antibody Test (Wondfo Biotech Co., Guangzhou, China), which assesses both IgG and IgM

198 antibodies against SARS-CoV-2. More details on the study protocol are available elsewhere(4).
199 For the present analysis, individuals with inconclusive test results were excluded.

200 **2.3.2. Official statistics data**

201 Official statistics data were collected from a dashboard by the Health Secretariat of Rio Grande
202 do Sul website (<https://covid.saude.rs.gov.br/>) for the period between February 29, 2020 (the
203 day of the first confirmed case in the State) and February 28, 2021. All 497 city-level health
204 secretariats in Rio Grande do Sul provide information daily on several indicators relevant for
205 monitoring the pandemic in the state, and this information is publicly available per day and per
206 city. We used the daily absolute number of new deaths attributed to COVID-19 as an indicator
207 of the relative temporal distribution of infections in the State. As discussed above, this is only
208 valid under the assumption that fatality is constant over time. We also obtained the daily
209 absolute number of confirmed infections to calculate the cumulative prevalence of confirmed
210 infections for comparison with our corrected estimates.

211 The cities included in the survey have different population sizes, but all received the same
212 weight in the study (see below for a justification for this). Therefore, weights for each city were
213 generated for the official statistics dataset as the multiplicative inverse of the number of
214 deaths in the corresponding city. This ensures that the distribution of deaths in each city has
215 the same weight in the overall distribution of deaths. A similar weighting scheme was used
216 when calculating the cumulative prevalence of confirmed infections.

217 **2.4. Statistical analysis**

218 **2.4.1. General description**

219 The goal of the analysis is to combine different data sources to obtain a plausible temporal
220 description of the cumulative prevalence of SARS-CoV-2 infections in Rio Grande do Sul. The
221 main difficulty is that, in the first eight EPICOVID19-RS surveys, only the Wondfo test was used,
222 while both Wondfo and ELISA tests were used. The difficulty stems from the fact that,
223 according to validation studies, the sensitivity of the Wondfo test decreases over time(7).
224 Therefore, any Wondfo seroprevalence estimate after the very beginning of the pandemic is
225 likely to be an underestimate in comparison to the ELISA test.

226 It is in principle possible to use the results from the validation study to account for this
227 temporal decay in sensitivity, so that sensitivity is assumed to be smaller in later surveys based
228 on some indicator of the temporal distribution of the epidemic, and therefore correction
229 procedures will have a stronger impact on estimates from later surveys. In the 9th survey, the
230 Wondfo seroprevalence was $\frac{92}{4499} \approx 2.04\%$, while the ELISA seroprevalence was $\frac{443}{4445} \approx 9.97\%$.
231 This difference in estimated seroprevalence is not compatible with our validation study,
232 suggesting that sensitivity of the Wondfo test in the field was lower than in the validation
233 study (possibly to the lower prevalence of highly symptomatic and/or severe infection cases in
234 the field, which could influence seroconversion and duration of antibodies over time)(13).

235 Therefore, the analysis requires two main steps:

- 236 a) Calibrating the results from the validation study so that the sensitivity it provides for the 9th
237 survey corresponds to the observed sensitivity, itself estimated by comparing the Wondfo
238 and ELISA estimates in the 9th survey (this simplified procedure for estimating sensitivity is
239 justified below).

240 b) Use the indicator and the calibrated temporal decay in sensitivity to obtain corrected
241 estimates for surveys 1-8. These corrected estimates can be interpreted as the expected
242 estimates had ELISA been used.

243 We now describe each one of these steps in detail.

244 **2.4.2. Calibrating the temporal decay in sensitivity**

245 The validation study (details on study design are provided in the Supplement) had data on the
246 date of diagnosis by RT-PCR and of testing by the Wondfo test (thus yielding the time between
247 diagnosis and testing), but not of symptom onset. Therefore, the validation study was re-
248 analyzed in each iteration of the correction procedure. In each iteration:

- 249 • The validation study data was resampled without replacement. This allows incorporating
250 sampling variability in the validation study itself as in a non-parametric bootstrap
251 procedure.
- 252 • T_2 and T_5 values were generated and added to the time between diagnosis and testing in
253 the resampled dataset to generate t^* .
- 254 • A model for the change in sensitivity over time was then fitted by an automated model
255 selection procedure (see the Supplement for details).
- 256 • Since the validation study lacked data on sensitivity of the Wondfo test for recent
257 infections, extrapolation for the smallest value of t^* in the dataset to $t^* = 0$ was required.
258 However, the observed data does not capture the increase in sensitivity during the first
259 days following infection. This gap in the range of t^* was imputed by assuming that
260 sensitivity from $t^* = 0$ (assumed to be 1%) to the smallest value of t^* (using the predicted
261 sensitivity from the model) in the given iteration has a logit-linear relationship.

262 The process above generated (in each iteration) $\hat{g}'(t^*)$, which is the function describing how
263 sensitivity decreased over time in the validation study. As discussed above, the observed
264 differences in seroprevalence estimates from the Wondfo and ELISA tests in the 9th survey
265 were not compatible with our validation study. To account for this difference, we calibrated
266 $\hat{g}'(t^*)$ into $\hat{g}(t^*) = r[\hat{g}'(t^*)]$, where $0 < r < 1$.

267 The calibration procedure was performed by finding the value of r using a one dimensional
268 optimization algorithm such that $\bar{D}(t_9)$ (where t_9 is the date of the 9th survey) is virtually
269 identical to $\frac{\hat{\rho}_{W_9}}{\hat{\rho}_{E_9}} \approx 20.52\%$ (where ρ_{W_9} and ρ_{E_9} respectively denote the seroprevalence as
270 measured by the Wondfo and ELISA tests in the 9th survey), which is an estimate of the
271 sensitivity of the Wondfo test in the 9th survey. This process ensures that $\bar{D}(t_9)$ is (virtually)
272 identical to the sensitivity in the last survey, thus making $\hat{g}(t^*)$ and field estimates of
273 sensitivity more compatible.

274 Importantly, this calibration procedure is arbitrary because many other transformations of
275 $\hat{g}'(t^*)$ could be used. We decided to simply scale $\hat{g}'(t^*)$ by a multiplicative constant because
276 this is a simple procedure that is rank preserving, therefore retaining the overall trends of the
277 original function. However, the calibration procedure is entirely numerical, thus being agnostic
278 to biological considerations. Nevertheless, the calibration does return a sensitivity curve that is
279 at least compatible to field estimates, which is the goal of the calibration procedure.

280 **2.4.3. Correcting the Wondfo estimates from surveys 1-8**

281 As described above, the temporal distribution of deaths was used as an indicator of the
282 temporal distribution of the epidemic. However, because the official statistics dataset does not
283 have data when infection occurred (which is indeed virtually impossible to ascertain), the
284 correction procedure was implemented as an iterated process. In each iteration, T_2 values
285 were generated and subtracted from the date at symptom onset (available in the official
286 statistics dataset), thus yielding the infection date t .

287 To calculate corrected cumulative prevalence estimates (denoted by $\hat{\rho}_{E_k}$) in surveys 1-8,
288 sensitivity (denoted by $\bar{D}(t_k)$) was calculated as the weighted average of $\hat{g}(t^*)$ over the period
289 from February 29, 2020 to the given survey, where the weight that each date receives is the
290 sum of the weights (described in section 2.3.2) of all deaths with infection occurring in the
291 given date. $\bar{D}(t_k)$ was then applied to the following formula: $\hat{\rho}_{E_k} = \frac{\hat{\rho}_{W_k}^{-(1-\hat{\epsilon}_k)}}{(\bar{D}(t_k) + \hat{\epsilon}_k - 1)}$, (14) where
292 ρ_{E_k} and ρ_{W_k} denote the seroprevalence as measured by the ELISA and Wondfo tests
293 (respectively) in the k th survey; and $\hat{\epsilon}_k$ is the specificity of the Wondfo test in the k th survey.
294 We assumed $\hat{\epsilon}_k = 1$ in all surveys, so the formula simplifies to $\hat{\rho}_{E_k} = \frac{\hat{\rho}_{W_k}}{\bar{D}(t_k)}$.

295 The strategy outlined above assumes that specificity of the Wondfo test is 100%. Although this
296 is a strong assumption, it can be justified in this context as follows. First, $1 - \hat{\rho}_{W_1} = 1 -$
297 $\frac{2}{4149} \approx 99.95\%$, which is a lower bound for the test's specificity since it was applied in the
298 field. Second, although we have no data on how specificity changes over time, it is likely to
299 increase because the sensitivity decreases. Therefore, $\hat{\epsilon}_k = 1$ is likely a good approximation in
300 this situation, which justifies estimating $\bar{D}(t_9)$ as $\frac{\hat{\rho}_{W_9}}{\hat{\rho}_{E_9}}$, simplifies the formula for calculating $\hat{\rho}_{E_k}$
301 and prevents it from yielding negative values. Although the formula could still yield $\hat{\rho}_{E_k}$ values
302 larger than 100%, this cannot happen in the current application because $\max(\hat{\rho}_{W_k}) = \hat{\rho}_{W_9} \approx$
303 2.04% and $\min(\hat{\rho}_{E_k}) = \bar{D}(t_9) \approx 20.52\%$, and $\frac{2.04}{20.52} \approx \hat{\rho}_{E_9}$. We also performed a subset of the
304 analysis using a likelihood-based approach (described in detail elsewhere(15)) and obtained
305 very similar results.

306 Confidence intervals of the corrected estimates for surveys 1 to 8 incorporated the different
307 sources of uncertainty in a bootstrap procedure (see Supplement for details). All analyses were
308 performed using R 4.0.2.

309 3. RESULTS

310 Table 1 displays the results of the simulation study. In comparison to the apparent prevalence,
311 corrected prevalence estimates were on average much closer to the true prevalence.
312 Corrected estimates were slightly biased upwards, but both bias and absolute deviation (that
313 is, the average absolute distance from the true prevalence) were of small magnitude.

314 Figure 1 shows the cumulative prevalence of infections. The solid line represents the
315 cumulative prevalence of confirmed infections. Estimates from the Wondfo test were not only
316 substantially smaller than corrected estimates (especially for later surveys), but also presented
317 a different overall pattern that would not resemble the remaining results even upon scaling.
318 Moreover, Wondfo estimates were implausible when compared to the cumulative prevalence
319 of infection according to official cases. Up to the 8th survey, the Wondfo and official cumulative
320 prevalence estimates were similar in the additive scale, but in the 9th survey the Wondfo
321 estimate was substantially smaller than the estimate from official statistics, which is a lower

322 bound of the true cumulative prevalence. Table 2 shows the seroprevalence estimates for each
323 survey of the EPICOV19-RS study using the different methods.

324 4. DISCUSSION

325 In this work, we combined data from official statistics, a series of nine population-based
326 serological surveys and a validation study to estimate the cumulative prevalence of SARS-CoV-
327 2 infection in the State of Rio Grande do Sul (Southern Brazil) by adjusting estimates from a
328 rapid test into the expected result had the ELISA test been used instead. Corrected estimates
329 are likely more plausible than estimates using the rapid test, especially when compared to
330 confirmed cases from official statistics. The corrected result indicated that, as of late February
331 2021, cumulative prevalence of confirmed cases corresponds to about half of all cases
332 detected by ELISA.

333 Describing the temporal evolution of the epidemic is important for several reasons. First, the
334 true number of infections is required for calculating several important quantities important for
335 policy making, including fatality and hospitalization rates(16). Second, an accurate estimate of
336 the temporal distribution allows better calculation of quantities required for projections using
337 models of infection dynamics, such as the basic reproduction number and how it changes over
338 time, especially after specific events such as lockdown measures or social events that may lead
339 to overcrowding. Projections from disease dynamics models early in the pandemic were highly
340 influential and were one of the few sources of information then available. Although important
341 and useful, it must be noted that most early projects were necessarily based on preliminary
342 estimates from other diseases or from small, non-representative studies. Moreover, it is
343 difficult to *a priori* identify and incorporate all possible complex factors that may influence the
344 temporal evolution of the epidemic, many of which are local and difficult to measure. One year
345 after the first confirmed case in Rio Grande do Sul, there is substantial local data available
346 from official statistics and the EPICOV19-RS study, thus allowing comparing initial projections
347 to the real figures to refine future projection models, which can now use local, real-data
348 estimates.

349 The study has considerable strengths. First, the EPICOV19-RS study is a unique resource that
350 includes nine population-based seroprevalence surveys covered a period of about 10 months
351 and begun shortly after the first confirmed case in the State. Second, the distribution of all but
352 one of the transition times was based on local data. Third, the fact that both the rapid and the
353 ELISA tests were used in the 9th survey allowed us to calibrate the sensitivity function with a
354 result obtained in the field. Fourth, corrected results were more plausible than uncorrected
355 estimates, which underestimated even the cumulative prevalence of confirmed cases after the
356 8th survey.

357 An important limitation of the study is the need of many assumptions throughout the
358 correction process, including: fatality ratio is constant over time; and the sensitivity function
359 estimated in the validation study (which was enriched for symptomatic cases) is applicable to
360 the field (which includes the general population) after a calibration procedure. It is not
361 possible to empirically verify the assumption of constant fatality over time without making
362 additional assumptions that may lead to circular reasoning. Regarding the sensitivity function,
363 its validity can only be assessed by repeatedly applying the rapid test over time to individuals
364 sampled from the general population who had been diagnosed with known date. Establishing
365 such cohort would be logistically difficult and time consuming, requiring large initial sample
366 sizes to identify enough infected individuals. It should also be mentioned that the ELISA test is

367 itself not perfect. Indeed, there is evidence indicating that some individuals do not
368 seroconvert, and this may be associated with disease severity(13). Therefore, estimates
369 presented here must be interpreted as the cumulative prevalence of positive ELISA tests rather
370 than of true infections.

371 This study is not a definitive guide, but rather an example of the usefulness of integrating
372 different sources to correct estimates from an imperfect test to obtain a more plausible
373 temporal trend of the COVID-19 epidemic. Although the study demonstrates the practical
374 importance of analytical procedures, it also highlights the critical importance of good data,
375 including population-based estimates from initiatives such as the EPICOV19-RS study, which
376 ideally should be performed using appropriate tests; extensive validation studies evaluating
377 how different factors (such as time since diagnosis) can affect the test's performance; and
378 good quality, transparent and freely accessible official statistics. Estimates from large and
379 populationally-representative data sources with sufficiently fine temporal is the best way to
380 track the progression of the pandemic and to substantiate policy making, and therefore
381 obtaining such data should be supported by funders and governments.

382 REFERENCES

- 383 1. Sabino EC, Buss LF, Carvalho MPS, Prete CA, Crispim MAE, Fraiji NA, et al. Resurgence of
384 COVID-19 in Manaus, Brazil, despite high seroprevalence. *Lancet*. 2021;397(10273):452–5.
- 385 2. Correio do Povo. RS identifica nove casos da variante P.1 da Covid-19. 2021 [cited 2021
386 Mar 10]. Available from: <https://www.correiodopovo.com.br/noticias/geral/rs-identifica-nove-casos-da-variante-p-1-da-covid-19-1.575688>.
- 388 3. Governo do Rio Grande do Sul. RS em bandeira preta: veja o que muda em todas as
389 regiões a partir de sábado, dia 27 - Portal do Estado do Rio Grande do Sul. [cited 2021 Mar
390 10]. Available from: <https://www.estado.rs.gov.br/rs-em-bandeira-preta-veja-o-que-muda-em-todas-as-regioes-a-partir-de-sabado-dia-27>
- 392 4. Hallal PC, Horta BL, Barros AJD, Dellagostin OA, Hartwig FP, Pellanda LC, et al. Trends in
393 the prevalence of COVID-19 infection in Rio Grande do Sul, Brazil: Repeated serological
394 surveys. *Cienc e Saude Coletiva*. 2020;25(suppl 1):2395–401.
- 395 5. Silveira MF, Barros AJD, Horta BL, Pellanda LC, Victora GD, Dellagostin OA, et al.
396 Population-based surveys of antibodies against SARS-CoV-2 in Southern Brazil. *Nat Med*.
397 2020;26(8):1196–9.
- 398 6. Pellanda LC, da Ros Wendland EM, McBride AJA, Tovo-Rodrigues L, Ferreira MRA,
399 Dellagostin OA, et al. Sensitivity and specificity of a rapid test for assessment of exposure
400 to SARS-CoV-2 in a community-based setting in Brazil. *medRxiv*. 2020;doi:
401 10.1101/2020.05.06.20093476.
- 402 7. Silveira MF, Mesenburg M, Dellagostin OA, Oliveira NR, Maia MAC, Santos FDS, et al.
403 Time-Dependent Decay of Detectable Antibodies Against SARS-CoV-2: A Comparison of
404 ELISA with Two Batches of a Lateral-Flow Test. *SSRN Electron J*.
405 2021;doi:10.2139/ssrn.3757411.
- 406 8. Alvim RGF, Lima TM, Rodrigues DAS, Marsili FF, Bozza VBT, Higa LM, et al. An affordable
407 anti-SARS-COV-2 spike protein ELISA test for early detection of IgG seroconversion suited
408 for large-scale surveillance studies in low-income countries. *medRxiv*. 2020;doi:
409 10.1101/2020.07.13.20152884.
- 410 9. Qin J, You C, Lin Q, Hu T, Yu S, Zhou XH. Estimation of incubation period distribution of

- 411 COVID-19 using disease onset forward time: A novel cross-sectional and forward follow-
412 up study. *Sci Adv.* 2020;6(33):1202–16.
- 413 10. Dhouib W, Maatoug J, Ayouni I, Zammit N, Ghammem R, Fredj S Ben, et al. The incubation
414 period during the pandemic of COVID-19: a systematic review and meta-analysis. *Syst Rev.*
415 2021;10(1):1–14.
- 416 11. Borremans B, Gamble A, Prager KC, Helman SK, McClain AM, Cox C, et al. Quantifying
417 antibody kinetics and rna detection during early-phase SARS-CoV-2 infection by time since
418 symptom onset. *Elife.* 2020;9:1–27.
- 419 12. Herrington D, The COVID-19 Community Research Partnership Study Group. Duration of
420 SARS-CoV-2 Sero-Positivity in a Large Longitudinal Sero-Surveillance Cohort: The COVID-19
421 Community Research Partnership. *medRxiv.* 2021;10.1101/2021.01.27.21250615.
- 422 13. Van Elslande J, Oyaert M, Ailliet S, Van Ranst M, Lorent N, Vande Weygaerde Y, et al.
423 Longitudinal follow-up of IgG anti-nucleocapsid antibodies in SARS-CoV-2 infected
424 patients up to eight months after infection. *J Clin Virol.* 2021;136:104765.
- 425 14. Ahlbom A. *Introduction to Modern Epidemiology.* Chestnut Hill, MA, USA: Epidemiology
426 Resources; 1984. 97 p.
- 427 15. Hallal PC, Hartwig FP, Horta BL, Silveira MF, Struchiner CJ, Vidaletti LP, et al. SARS-CoV-2
428 antibody prevalence in Brazil: results from two successive nationwide serological
429 household surveys. *Lancet Glob Heal.* 2020;8(11):e1390–8.
- 430 16. Gaye B, Fanidi A, Jouven X. Denominator matters in estimating COVID-19 mortality rates.
431 *European Heart Journal.* 2020;41(37):3500.
- 432

433 **TABLES**

434

435 **Table 1. Performance of the correction procedure in the simulation study (averaged over**
436 **1000 datasets).**

<i>t</i>	True prevalence ^a	Apparent prevalence ^b	Corrected values		
			Prevalence ^c	Bias ^d	Absolute bias
60	0.011%	0.002%	0.014%	0.003 pp	0.022 pp
120	0.300%	0.093%	0.307%	0.007 pp	0.114 pp
180	2.383%	0.988%	2.408%	0.025 pp	0.274 pp
240	6.503%	3.051%	6.518%	0.015 pp	0.416 pp

437 ^aTrue cumulative prevalence of infections.

438 ^bCummulative prevalence of infections estimated using a test with decaying sensitivity.

439 ^cCummulative prevalence of infections estimated by the correction procedure.

440 ^dDifference between true and corrected prevalence.

441 pp: Percent points.

442

443 **Table 2. Seroprevalence (%) estimates (95% confidence intervals) in Rio Grande do Sul for**
444 **each survey.**

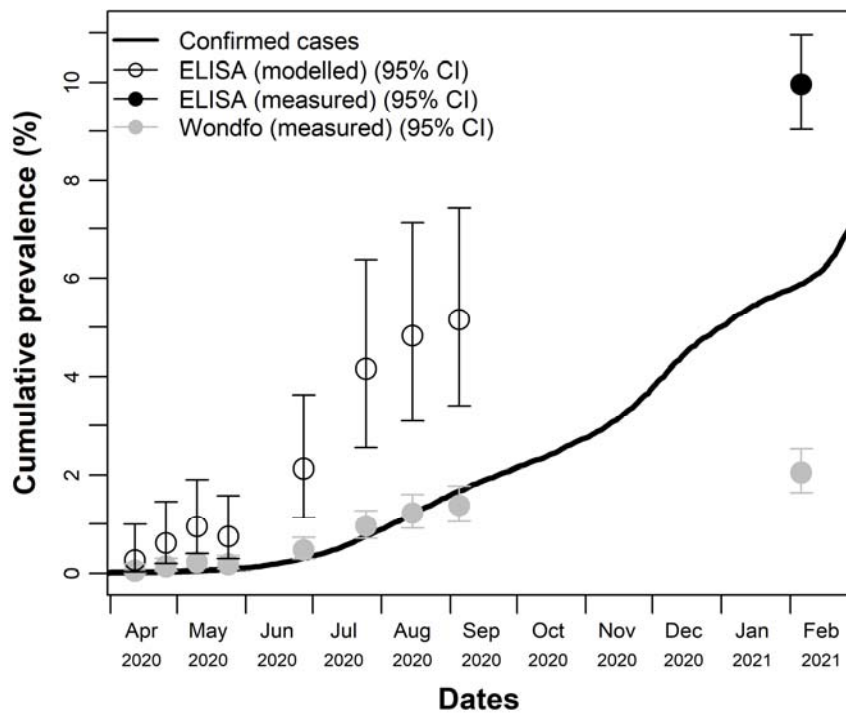
Survey	Wondfo		ELISA	
	Method	Values	Method	Values
1	Measured	0.05 (0.01-0.17)	Modelled	0.26 (0.03-1.00)
2	Measured	0.13 (0.05-0.29)	Modelled	0.61 (0.19-1.45)
3	Measured	0.22 (0.11-0.41)	Modelled	0.94 (0.39-1.90)
4	Measured	0.18 (0.08-0.35)	Modelled	0.74 (0.28-1.58)
5	Measured	0.47 (0.28-0.72)	Modelled	2.12 (1.12-3.62)
6	Measured	0.96 (0.70-1.27)	Modelled	4.15 (2.55-6.36)
7	Measured	1.22 (0.91-1.60)	Modelled	4.82 (3.09-7.12)
8	Measured	1.38 (1.05-1.77)	Modelled	5.15 (3.40-7.43)
9	Measured	2.04 (1.64-2.52)	Measured	9.97 (9.03-10.96)

445

446 **FIGURE**

447

448 **Figure 1. Cumulative prevalence of SARS-CoV-2 infection (according to the ELISA test) in Rio**
449 **Grande do Sul (Southern Brazil) from February 29, 2020 to February 28, 2021.**



450